
Article:
Beagles, A. and Fletcher, D. (2013) The aerodynamics of freight; approaches to save fuel by optimising the utilisation of container trains. Proceedings of the Institution of Mechanical Engineers, Part F: Journal of Rail and Rapid Transit, 227. 635 - 643. ISSN: 0954-4097

https://doi.org/10.1177/0954409713488101

The aerodynamics of freight; approaches to save fuel by optimising the utilisation of container trains

Adam E Beagles*, David I Fletcher, The University of Sheffield, UK

*Corresponding author: Dr Adam Beagles: a.beagles@sheffield.ac.uk
Tel mobile: +44 (0) 7936412015
Tel direct: +44 (0) 114 222 7743
MERail Railway Research Group
Department of Mechanical Engineering
University of Sheffield
Mappin Street
Sheffield
S1 3JD
UK

Abstract

Aerodynamic drag is approximately proportional to speed squared so the drag of slower moving freight trains has received less attention than that of higher-speed passenger trains. Key results of wind tunnel tests of European container trains were published in 1989 and are the basis for most assessments of drag of European container trains (American container trains usually have far higher drag due to double-stacking containers or transporting complete semi-trailers and were studied in research programmes at a similar time). The research reported here concerns a reappraisal of the European results and of more recent results obtained from the application of computational fluid dynamics

(CFD) modelling and the results of real world and wind-tunnel testing of the aerodynamics of container wagons. The paper presents empirical equations that can be used to predict the energy savings associated with different container-loading scenarios within a fixed length train and the energy required for carrying aerodynamic features such as baffles or fairings. Illustrative examples are provided using data measured during freight operations.

The effect on drag of side-winds and their speed distributions are included as are representative vehicle speed profiles. Most previous authors ignored both side-winds and end-effects; it is shown that the effects of these are opposite but of similar magnitudes so the results of these authors will be valid.

Keywords

Aerodynamics, Container train, Energy efficiency. Drag, Loading, Side wind

1 Introduction

This paper considers the aerodynamic forces acting on container trains. It provides a reappraisal of some key test results [1] that have been the basis of much analysis.

The aerodynamic drag is approximately proportional to the square of (relative) wind speed. A non-dimensional aerodynamic drag coefficient (ADC), *C*, is

commonly defined so that the longitudinal force (resisting motion) attributed to the aerodynamics, F_{aero}, satisfies

$$F_{aero} = C \cdot \left(\frac{1}{2} \cdot \rho \cdot A \cdot V_{rw}{}^2 \right) \qquad (1.1)$$

where ρ is the density of air (standard value is 1.225kg/m³ [2], but depends on pressure, temperature, and humidity), A is the (effective) area of the front of the train (a value of 10m² is commonly used), and V_{rw} is the speed at which the wind impacts the train (calculated from the speed and direction of both train and wind), see Fig 1.

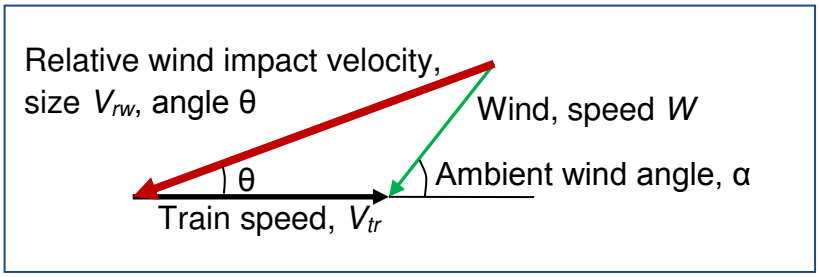

Fig 1: Definition of speeds and angles

The thesis by Vollmer [1] reported a large series of wind-tunnel tests: 1:32-scale models of a variety of freight vehicles were placed in a 40m/s wind and the forces they experienced were recorded at a range of angles to the incident wind. Using 21 different types of vehicles he tested 240 ‘trains’ consisting of between 1 and 8 vehicles rotated at various ranges of angles (recorded in 5°

increments so up to 72 angles per ‘train’) to the wind. For each configuration and angle he recorded three forces and three moments (in mutually orthogonal directions). He observed that the angular variation of each set of results could be well-approximated by only a few terms of a Fourier expansion in cosines; the sine terms are zero by symmetry. He thus reduced the 22 thousand measurements to a series of tables of Fourier coefficients (coefficients of $cos(2k\theta)$ for k=0,1,…,5, where θ is defined in Fig 1) that enable the lateral and longitudinal forces to be calculated for combinations of the vehicles at any angle to a wind. These tables have been used in many subsequent applications when aerodynamic drag was assessed, e.g. [3, 4, 5, 6]. However, subsequent work (discussed below) suggests that the testing method may have exaggerated the aerodynamic effect and the applications consider no cross-wind and generally ignore the vehicles’ speed profile. This work addresses these shortcomings and presents a methodology that can be used to determine more realistic approximations to the aerodynamic drag.

2 Test data and its use

Twelve multimodal wagon configurations relevant to this work were tested by Vollmer. They formed three series; illustrated in Fig 2.

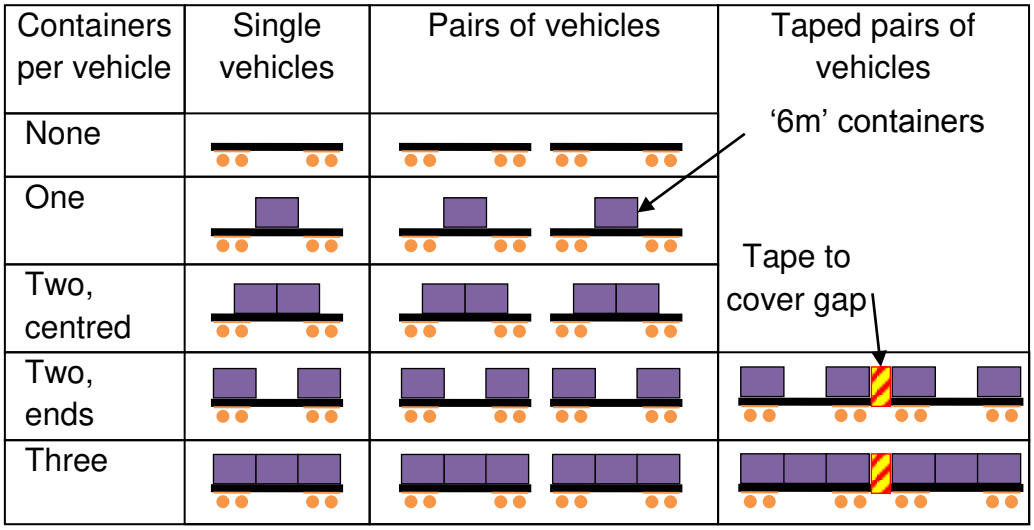

Fig 2: Container vehicles tested in wind-tunnel by Vollmer

2.1 Standard usage of test results

The results of these tests (the Fourier coefficients introduced above) can be used to predict the drag associated with freight trains consisting of multiple vehicles each carrying different numbers and sizes of containers. The simplest extrapolations of the testing are to consider adding additional identical vehicles; In all previous work the effect of adding any one vehicle into a rake of similar vehicles was considered to be the same as adding the second vehicle of a pair (Vollmer's tables include data for the difference between pairs of vehicles and single vehicles instead of the raw data for pairs of vehicles).

Two methods for calculating the drag associated with a vehicle that is different to the others in a rake (or, for container trains, the drag associated with an

unloaded vehicle in a train of loaded ones or vice-versa) have been proposed and are illustrated for the case of adding an unloaded container vehicle (frontal area 4.324m²) into a rake of fully loaded container vehicles (frontal area 9.361m²) with no cross-wind:

- Vollmer proposed that an additional term proportional to the difference in frontal areas be added, with the constant determined from his wind-tunnel tests being 312.5 km^{-2}. The additional ADC for the illustration would thus be $312.5 \cdot (9.361 - 4.324) \cdot 10^{-6} = 0.00157$

- Wende in his popular German textbook [3] uses results that Vollmer obtained by comparing the drag associated with taped pairs of vehicles (see Fig 2) with twice the results obtained from single vehicles (Vollmer postulated that the difference was attributable entirely to the interface). Wende proposes that the additional ADC is obtained by multiplying this "*Stirn/Heckkomponente*" (Front/rear component) of Vollmer's by the fractional change in frontal area. For the illustration the "*Stirn/Heckkomponente*" is 0.002338 so the additional ADC is $0.002338 \cdot \frac{9.361}{9.361 + 4.324} = 0.0016$; in this case very close to Vollmer's result above.

In either case the additional drag is taken to be zero if the extra vehicle is at the end and not as tall as the preceding vehicle.

In the standard usage, since the frontal areas of container vehicles carrying any number of containers (other than none) are the same, no additional drag is associated with the gaps between vehicles carrying different numbers of containers.

2.2 Proposed usage of test results

For this work we wanted to produce equations that could be used by freight operators to assess how best to load a train of a fixed length (and the energy associated with different loading choices), i.e. a train with a fixed number of wagons which is loaded by a variable number of shipping containers. In this scenario the drag associated with the wagons and the effect of additional wagons is not important; the train's consist is not being changed and it has a path reserved so the engine(s) will need to produce enough energy to move the wagons regardless of how they are loaded. Approximations to the drag attributable to the containers and their locations, was given by the differences between the ADC associated with the laden and unladen wagons (i.e. we subtracted the Fourier coefficients associated with the first row of tests indicated in Fig 2 from those associated with subsequent rows). The underlying assumption is that the drag associated with the deck structure and bogies is

unaffected by the number of containers on the deck; the major drag is associated with the flow around the bogies and this is isolated by the deck from that around the containers.

The influence of each container on the drag can be considered to be the sum of two components: one due to its length (air flowing past rough surfaces); and one due to its ends (front pressure, rear suction, and turbulence). However, for the analysis, the influence of the ends of consecutive containers is combined into a gap effect (which will be zero if the containers abut and there is no gap). Note that adding a container at the end of a train (after what had been the 'end' container) will introduce one gap and a length of container, while adding one in any other position will replace a large gap with two smaller gaps and a length of container. In deriving the equations for ADC in this paper we considered the effect on ADC of changing loading; for example, the ADC associated with the second container on the pair of vehicles with one container per vehicle (in Fig 2 the arrow from "'6m' containers" points to this container) was considered to result from the effect of an additional length of 6m and a 15m gap (the vehicle length across buffers was 21m).

It is normal when analysing the drag associated with the sides of a cylinder to consider drag to be proportional to length. Since containers are rectangular prisms we assume that the contribution to the ADC attributable to container

length is a term proportional to the length. We also assume that the contribution of gaps to the ADC takes the form of a decaying exponential function (see Equation (3.1), below). This form of dependency: is considered to be physically realistic; was used to approximate the wind-tunnel tests in [7]; gives a good approximation to the data in [8], and implies that it is always better that containers are placed adjacent to each other.

A benefit of our novel interpretation of Vollmer's data is that the drag associated with wheels and bogies is not used (we only work with differences between vehicle loading configuration and it is assumed that the effects associated with these identical parts are cancelled in finding the difference). This is beneficial since this drag is considered to be most prone to modelling errors due to: uncertainties associated with the boundary layer at rail level (testing was carried out on stationary vehicles); and the detail of the bogie structures on track being different to that in the tests.

3 Drag when there is no side-wind

The drag associated with adding containers to an unladen vehicle, calculated using Vollmer's data for no side-wind, is shown in Fig 3.

Perhaps the most interesting aspect of this plot is that the drag reduces as the container length increases. This is a feature of the results and indicates that the

relatively smooth surfaces of shipping containers are associated with less drag than the ribs on the deck of the wagon (which gets covered by the containers). Another point to note is the drag associated with a 9m gap: This is below the trend-line whereas it would be expected that the drag associated with a gap of this size would be closer to that for the 15m gap (according to [9] gaps longer than about 2m cause no more drag than a 2m gap).

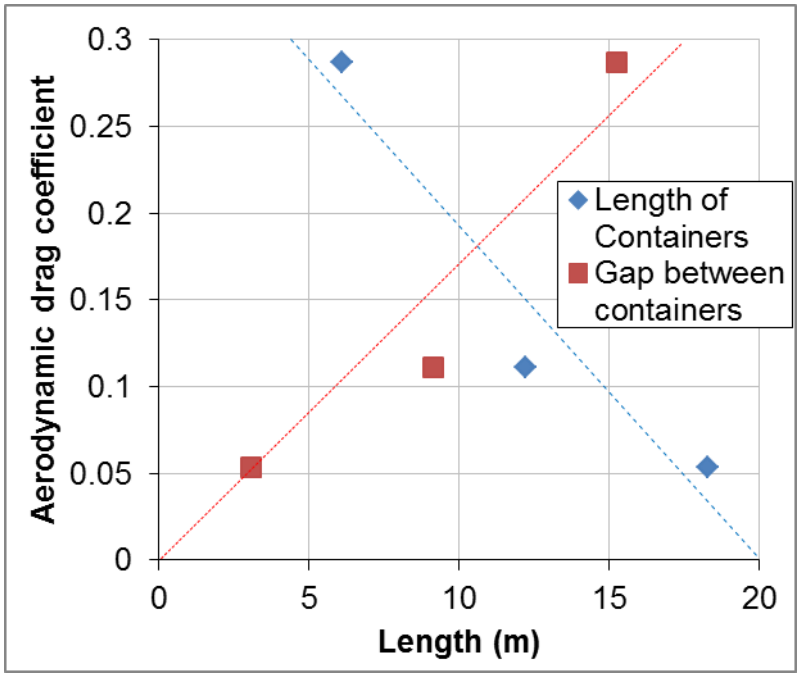

Fig 3: Aerodynamic drag coefficients showing trends with changing gap length and container length

A best fit using the decaying exponential function (as discussed in Section 2.2) of the length of the gap between containers, *G*, and a linear dependence on container length, *L*, is

$$C = 0.4 \cdot \left(1 - e^{-0.081 \cdot G}\right) - 0.003 \cdot L \qquad (3.1)$$

where *L* and *G*, are both in m. Note that the coefficient of *L*, being negative, is consistent with the observation on Fig 3 above. The coefficients in this expression were found by minimising the sum of the squares of the differences between the approximations and the values obtained from Vollmer's data.

The measurements reported by Vollmer were made with individual vehicles and pairs of vehicles so do not satisfy the requirements of more recent testing standards; e.g. [10] requires that "Freight wagons which can possibly run behind an empty flat wagon shall be tested using an empty standard two-axle container trailer model as upstream body". It has been found that the closer a feature is to the front of a train the larger the affect it will have on aerodynamic drag (e.g. [7, 8, 11]). It is proposed by reference to the results in these papers (see e.g. Fig 7 below) that the ADC in equation (3.1) should be reduced by an 'end-factor' of 3 (for the case in which there is no side-wind), this factor being derived in Section 4.3.

As an example of applying the above equations consider adding a standard 6m container to fill a 6m gap between two others (this is the 'good' position shown in Fig 9 below). This addition will increase the length of containers being carried (*L*) by 6m and remove a gap of length (*G*) 6m. The net effect is to reduce the ADC in equation (3.1) by $\frac{1}{3}\cdot\left(0.4\cdot\left(1-e^{-0.081\cdot 6}\right)+0.003\cdot 6\right)$ = ⅓(0.154+0.018) = 0.045. From equation (1.1), for a train travelling at 120kph (75mph) this is equivalent to a force of 0.31kN, so travelling for 100km there would be a saving of 31MJ of energy (neglecting the additional mass that would be being carried) through removing the gap by adding an additional container in its place. Had the same container been placed two vehicle-lengths behind a container (with no containers behind it) the drag would have increased and the additional energy for the same journey would have been 93MJ. So, in this example, the energy saving associated with an optimum container position would be 31+93=124MJ/100km.

4 Drag when there is a side wind

The previous Section considered only conditions without a side-wind (α=0 or π in Fig 1). When there is a side-wind the drag increases due to two effects: the wind impinging on additional leading surfaces; the vehicle being blown sideways causing either flange contact or additional creepage at the wheel-rail

contact. The former effect is included in the results of Vollmer [1], while for the latter it has been suggested [3] that the additional longitudinal force due to the lateral force, F_{long_lat}, is

$$F_{long\_lat} = \frac{1}{2} \cdot \mu \cdot F_{lat} \tag{4.1}$$

where μ is the rail-wheel coefficient of friction and F_{lat} is the lateral force (this can be calculated using results from Vollmer for lateral ADC and an equation similar to (1.1)). Relevant data is considered in the following Sections.

Another consequence of side winds is that the reduction in longitudinal ADC associated with the tests being on end vehicles becomes less significant (recall that an end-factor of a third was proposed for no side-wind in Section 3).

4.1 Effect of wind angle on longitudinal ADC

The Fourier expansions developed by Vollmer [1] to calculate the effect of wind angle on longitudinal ADC were used to calculate the data points shown in Fig 4.

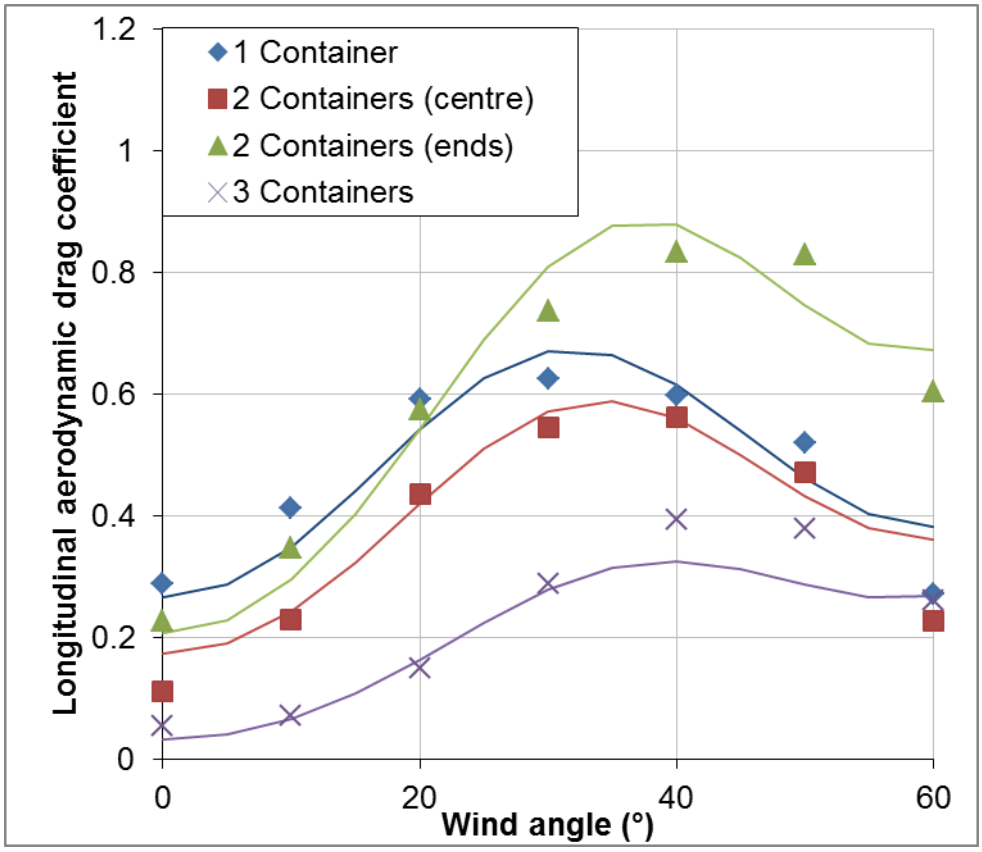

Fig 4: Variation of (longitudinal) ADC with angle of wind and approximations (solid curves) when indicated containers are added to a train in locations shown in Fig 2

It can be seen from Fig 4 that the peak ADC for the centrally loaded containers occurs at angles that increase with number of containers. This is consistent with the wind being able to impact the front face of a gap (for a figurative explanation see Fig 5).

The approximations shown as solid lines in Fig 4 were obtained by fitting curves of the form of equation (3.1) so that the ADC associated with a container subject to a side-wind at an angle θ (radians) can be approximated by

$$C_{Long} = (0.56 - 0.16 \cdot cos(6 \cdot \theta)) \cdot \left(1 - e^{(0.919 \cdot cos(\theta) - 1) \cdot G}\right) - 0.003 \cdot L \qquad (4.2)$$

The approximations become inaccurate for angles above about 60°, but such angles will only be relevant when vehicles are moving more slowly (e.g. even for a wind speed of 20m/s (see Section 6.1 below) this angle can only be exceeded when trains move below 23m/s (51mph)); at lower speeds the aerodynamic drag, proportional to V_{rw}^2, will be less significant. At angles above 70º Vollmer's data implies negative ADC so it is reasonable to suppose that the data is not valid for these angles.

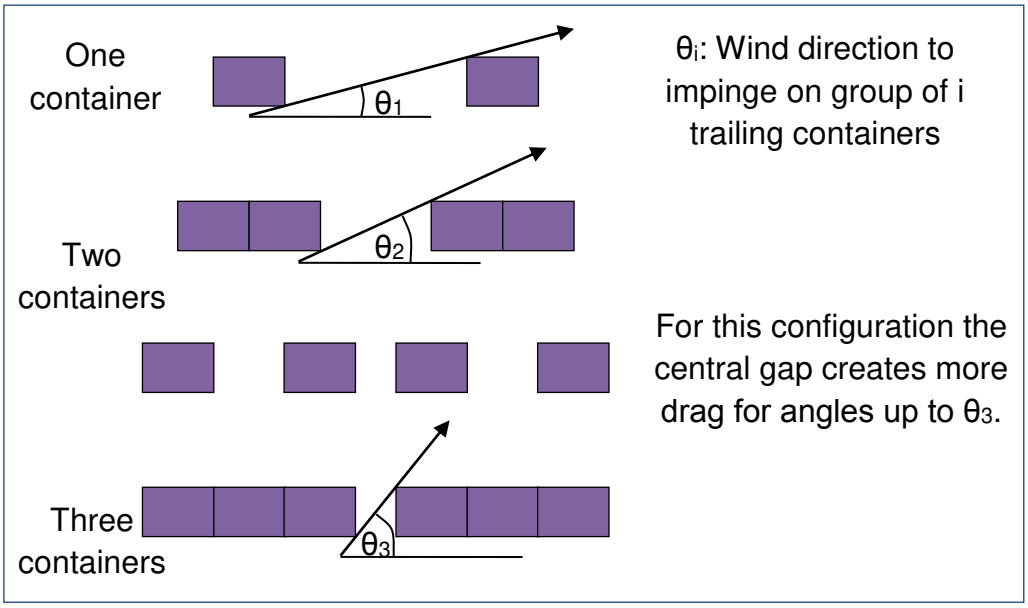

Fig 5: Effect of container spacing on aerodynamic drag in side-wind

4.2 Effect of wind-angle on lateral ADC

The Fourier expansions developed Vollmer [1] for the effect of wind-angle on lateral ADC were used to calculate the data points shown in Fig 6.

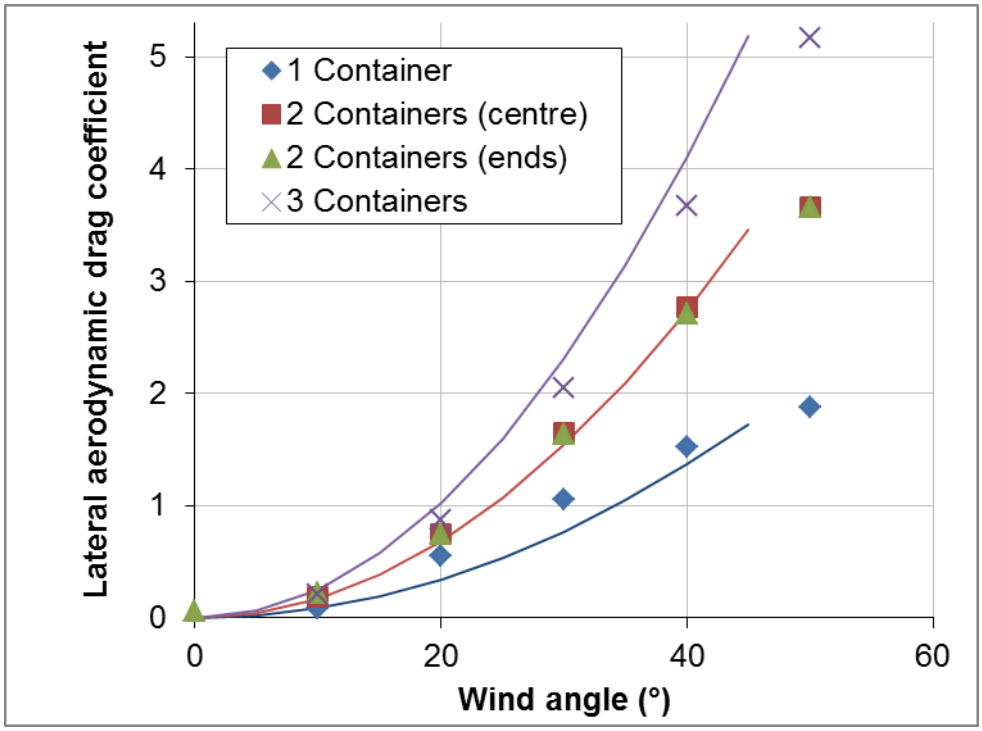

Fig 6: Variation of lateral aerodynamic drag coefficients with angle of wind and approximations (solid curves) when indicated containers are added to a train in locations shown in Fig 2

The results are as would be expected: there is a large lateral ADC that increases with angle of side-wind and becomes approximately proportional to the number of containers being carried. The approximations to the lateral ADC, C_{Lat}, are given by the following equation

$$C_{Lat} = 0.46 \cdot L \cdot \theta^2 \qquad (4.3)$$

4.3 End factor compensation for longitudinal ADC

As discussed in Section 3 the test results by Vollmer [1] are only for vehicles at the end of rakes (as they only included up to two vehicles). More recent experimental and numerical work (e.g. [7, 8, 11]) has shown that this will over-estimate the longitudinal ADC:

- The wind-tunnel testing in [7] considered the drag associated with gaps at different positions along a container train so is directly relevant to this work. The factor was calculated by dividing the drag for the first car into that for one remote from the beginning of the train.

- The wind-tunnel testing in [8] considered variations of open hopper wagons. The factors are the (average of positive and negative wind angle) ratio between the ADC associated with an end vehicle and that associated with a vehicle that has one and a half (!) vehicles in front of it; the author states that “only minor changes should occur for wagons positioned further along the train”.

- The CFD testing in [11] considered different positions of open cargo wagons. The results show high drag for front and rear vehicles and little variation for intermediate ones. The factors plotted in Fig 7 are the

average of the factors for the front and rear (ratio of ADCs for extreme and adjacent vehicles)

A correction was determined to agree with an upper bound to these more recent results. The data and approximation to it is shown in Fig 7.

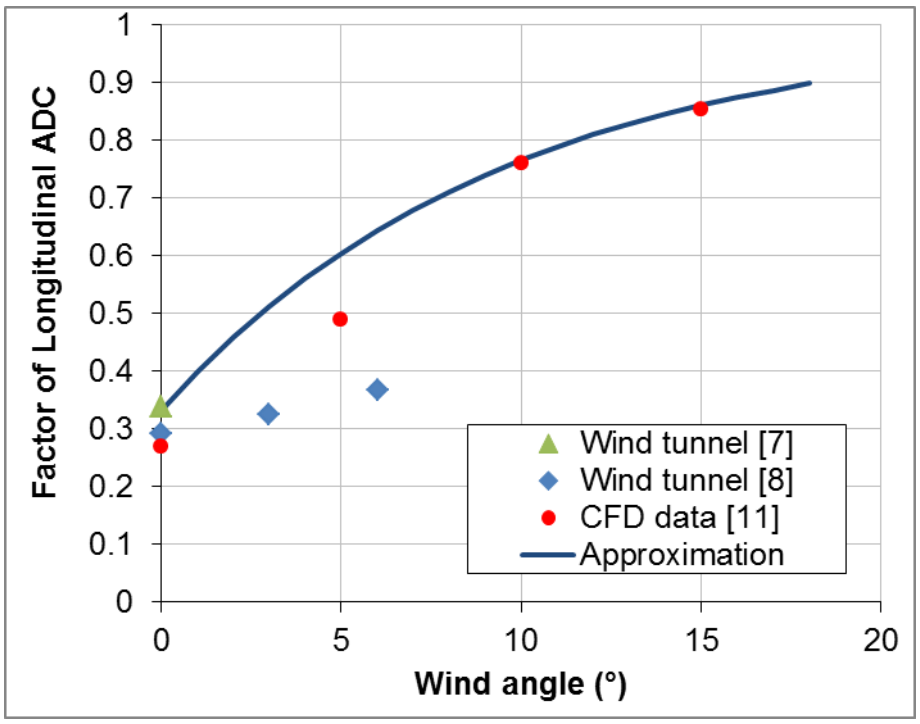

Fig 7: Correction factor (Red_{Long}) to be applied to longitudinal ADC to compensate for measurements being on only one or two vehicles

The approximation to the reduction, Red_{Long}, shown in Fig 7 has the equation

$$Red_{Long} = \frac{1 + 2 \cdot \left(1 - e^{-6 \cdot \theta}\right)}{3} \qquad (4.4)$$

Note that as we are considering changes in loading, the ADC associated with the end container (which would have Red_{Long}=1) is not relevant; there is assumed to always be an end container.

5 Total drag

The above equations can be combined to give the aerodynamic force resisting motion for a container loaded on an intermodal wagon as

$$F_{aero} = \left(Red_{Long} \cdot C_{Long} + \frac{1}{2} \cdot \mu \cdot C_{Lat}\right) \cdot \left(\frac{1}{2} \cdot \rho \cdot A \cdot V_{rw}{}^{2}\right) \qquad (5.1)$$

with C_{Long}, C_{Lat}, and Red_{Long} being defined by equations (4.2), (4.3), and (4.4) respectively; μ is the rail-wheel coefficient of friction; ρ is the density of air; A is 10m²; and V_{rw} is the wind speed relative to the train. C_{Long} is a function of the container length (L) and the gaps it creates when loaded on the train (G).

Note that the force due to lateral ADC is considered to be unaffected by container location (no Red_{Long} factor) since, unlike the longitudinal ADC, a container is not shielded from lateral air flow by preceding containers. Also, for the most common low wind angles the lateral ADC is very small (see Fig 6) so will not contribute significantly to the aerodynamic force.

Other forces that change when a container is loaded are the curving, acceleration, climbing, and the rolling resistance. The first three are

approximately proportional to weight, while the rolling resistance has a far more complicated dependence (see e.g. [3]). If it is assumed that a container of the same weight would have been loaded somewhere on the train then these forces would not vary significantly. The following sections consider the additional force associated with increasing mass, for example, through addition of features that are designed to reduce the aerodynamic drag.

5.1 Curving resistance

Equations for curving resistance assume the force is proportional to the reciprocal of radius (see e.g. [3, 4]). Various complicated expressions are given for the constant of proportionality (depending on the relevant wheel-rail contact angles, track cant, bogie wheel-base, suspension details, etc.), but a fixed value of about 700Nm is reasonably conservative (see table comparing international standards in [12]). Note that other studies [4, 5] state that the curving resistance is generally small and that it is too complicated to calculate.

5.2 Acceleration resistance

This force is given by the simple application of Newton's law.

5.3 Climbing resistance

This is the force required to lift the additional mass.

5.4 Rolling resistance

This resistance includes all factors not covered by the above, predominantly: friction and deformation losses at the wheel/rail contact (affected by material properties, surface roughness, differential wheel diameters, out-of-roundness of wheels); damping associated with track-bed deformation; and friction losses in roller bearings, couplers, and other moving parts of the vehicle.

Empirical relationships have been obtained expressing rolling resistance as a function of weight, axle-load, train length, and train speed (see e.g. [3]); an approximation is presented in [5] that is said to provide errors of only 2-4%. This approximation is presented as a table of linear functions of the form shown in equation (5.2)

$$F_{roll} = (A_r + B_r \cdot n_{axle}) + (C_r + D_r \cdot L_{tr}) \cdot V_{tr} \qquad (5.2)$$

where n_{axle} is the number of wagon axles, L_{tr} is the total length of the train, V_{tr} is the train speed, and A_r, B_r, C_r, and D_r are presented as constants, but apart from A_r (which appears to be approximately constant) they can be well approximated as linear functions of the mass being transported. The change in force due to additional mass can thus be estimated by using the coefficients of the mass in these linear functions. This procedure produces the following

equation for the rolling resistance, F_{roll} (N), associated with carrying a container of mass M (tonne):

$$F_{roll} = M \cdot \left(4.76 + \left(-0.43 + 0.02 \cdot L_{tr}\right) \cdot V_{tr}\right) \tag{5.3}$$

6 Relative Speeds

To use the equations for aerodynamic drag it is necessary to know the relevant speeds and directions of both wind and train.

6.1 Wind Speed

The wind speed data is available from the UK meteorological office and various weather stations at a height of 10m above ground level. Typical average values are around 4m/s; there are seasonal variations and larger values nearer the coast and further north. Extrapolating to values relevant to trains is a very complicated process as the effect of surface features and wind directions causes local wind speed variations (e.g. in a cutting or on an embankment, passing a building or a wood, the funnelling effect of valleys, etc.). Procedures for the calculation are outlined in two standards: [13], which provides a complex calculation for all local effects; and [10] which gives an overview of requirements for rail vehicles. These standards are mainly concerned with predicting the risks associated with extreme weather so it may not be appropriate to apply them to normal operation.

The wind speed experienced by the freight train that had its containers blown off at Cheddington on the West Coast Main Line [14] was calculated to be around 20m/s in a 'near gale' when allowing for gusts and the intensifying effect of a 4m embankment.

It is normally assumed (e.g. [15]) that the wind speed distribution can be approximated by a Weibull distribution with a shape parameter of about 1.7. With this assumption and an average speed of 4m/s, the probability of a wind speed exceeding 20m/s will be less than about 0.0003%.

6.2 Freight vehicle speeds

Speeds of freight trains are available from the on-train monitoring recorders (OTMR). Data for typical freight trains (for over three thousand km of running) was provided by Freightliner Ltd. The speed profile (cumulative fraction of speeds neglecting times when the train is stationary) is shown in Fig 8. It was found that, although the maximum speed of the vehicle is 33.5m/s (75mph), less than a quarter of the travelling was undertaken at speeds exceeding 60mph and the median speed was only 23m/s (51mph). This distribution was typical for all runs and the speeds are significantly below line speeds (e.g. the distribution of line speeds for representative sections of UK freight routes is shown in Fig 8 and has a median of 33m/s (74mph); this data is taken from [16]

and includes a significant part of the route followed by the monitored freight trains).

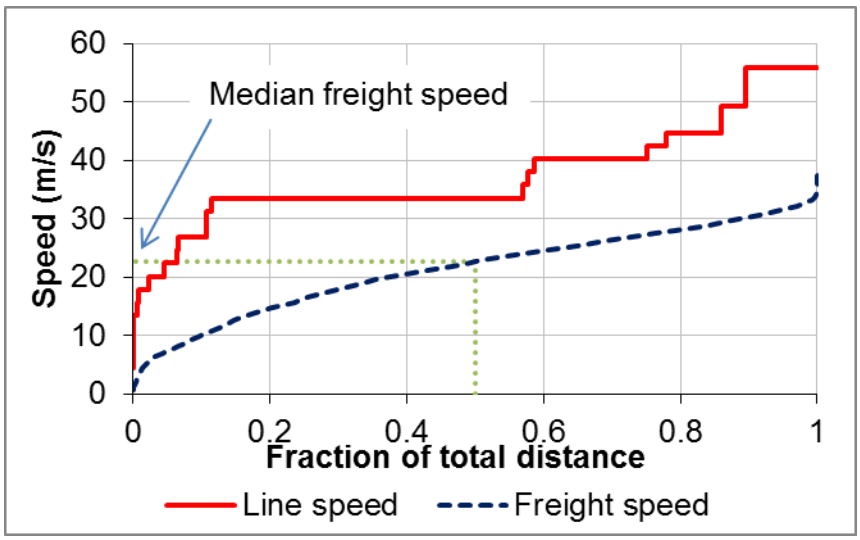

Fig 8: Variation of speed of freight train with distance travelled and lengths of line-speeds on freight routes

7 Application

The data above was used to calculate the energy savings that are associated with loading a container to minimise the aerodynamic drag (the difference between the 'poor' and 'good' positions shown in Fig 9 and discussed in Section 3). Note that the energy saved is calculated using a gap of zero for the 'good' position and the sum of the drag associated with 6m and 48m gaps for the 'poor' position.

The forces (and hence energy) were calculated as the average of the forces associated with winds that are equally probable to come from any direction (uniform distribution of α in Fig 1) and whose speed has a Weibull distribution with the indicated means. If the anticipated wind directions are known for a route they could be used, but, as mentioned in Section 6.1, the wind direction experienced at the train may differ significantly from that forecast and this (more arduous) calculation would be only be valid for the specific route and wind conditions.

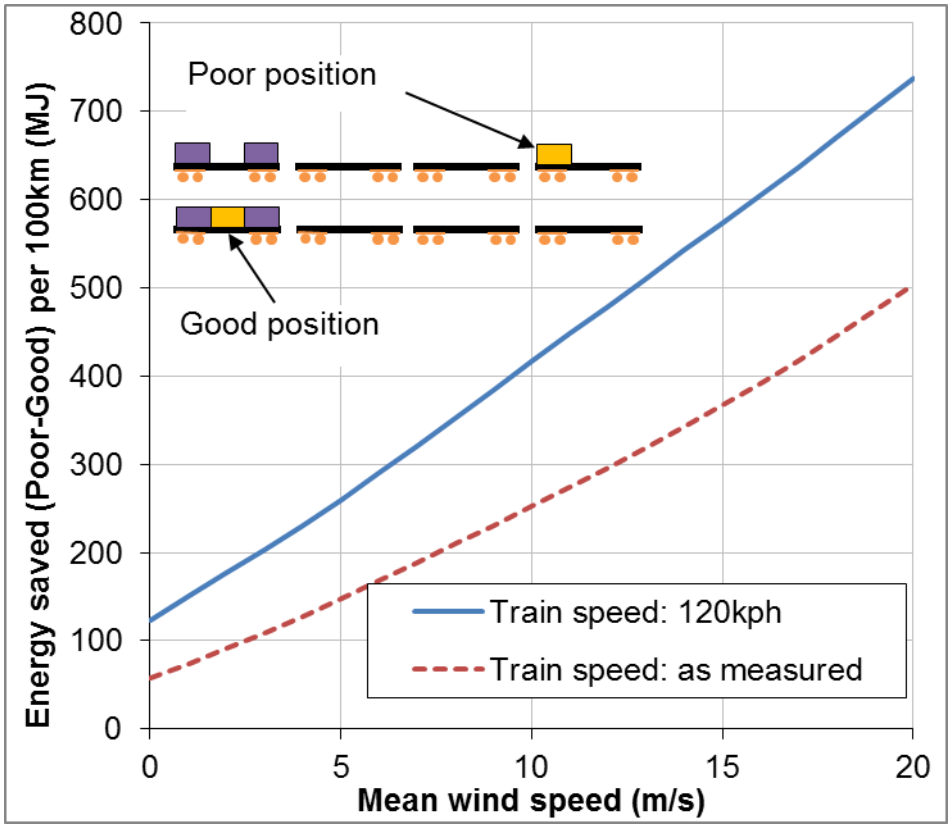

Fig 9: Energy that can be saved by optimal positioning of a container

In Fig 9:

- the 'Train speed: 120kph' curve assumes the train is traveling at a constant 120kph, while the 'Train speed: as measured' uses the 'Freight speed' distribution shown in Fig 8
- the zero wind speed point on the 120kph curve is the 124MJ calculated in Section 3

- the zero wind speed point on the measured speed curve (57MJ) compares well with the 45MJ predicted in [4] for aerodynamic energy consumption associated with measured speeds on a vehicle with a maximum speed of only 100kph (factoring 45MJ by speed squared would imply 65MJ)
- the energy consumption calculated at a mean wind speed of 4m/s (128MJ/100km) is a factor of 2¼ larger than that for zero wind speed (57MJ/100km) so the previous work (e.g. [3, 4, 5, 6]) that neglected both wind speed and train-end effects would not have been too inaccurate (as shown in Fig 7, end effects contribute a factor of about a third for a wind angle of 0º, so the error in results would be only about 1-2¼/3=25% and less than this if a higher mean average speed were appropriate)

The energy required for carrying aerodynamic features such as baffles or fairings can be calculated using the equations introduced in Section 5. The energy to transport a mass *M* (kg) (for example a device to reduce aerodynamic drag) along the studied route is given as

$$Energy = (0.028 + 0.253 + 0.001 + 2.069) \cdot M = 2.351 \cdot M \qquad \text{(MJ/100km)} \quad (7.1)$$

where the four numbers are the contributions from the four forces in the corresponding sub-section of Section 5. These values were calculated as follows:

- Curving resistance: the radii of track curves were derived from the trains OTMR, GPS, data; a numerical approximation to the best circular arc approximating a sequence of at least four points covering a distance of at least 10m was calculated.
- Acceleration resistance: the energy differences when the train had accelerated were summed (speeds from OTMR data); note that it is assumed that all braking energy is lost.
- Climbing resistance: the route gradients were obtained using data from Network Rail; it was assumed that all this energy was required to be provided by the locomotive
- Rolling resistance: the OTMR speed data was used with an assumed train length of 500m.

Comparing equation (7.1) with Fig 9 it can be seen that the energy saving associated with optimum positioning of a container is equivalent to that associated with transporting about 54kg less load.

8 Discussion

The novel approach presented here to analysing wind tunnel data (subtracting the effect of bogies and calculating the effect of changes in container position) assumes that the drag associated with bogies is independent of the load that is being carried by the wagon. This is considered to be a reasonable assumption, as any extrapolation from test data will be approximate but it is noted that there will be some flow through the deck of a wagon that will cause inaccuracies.

It was commented in Section 3 that the negative coefficient of container length indicated the reduced drag associated with the relatively smooth container sides compared with the bluff aspects of the deck. Adding a smooth covering to the deck may be beneficial; the mass of such a covering would always be transported, so it would need to be light. The ADC reduces by 0.003/m (Equation (3.1)) which, using Equation (1.1), equates to an aerodynamic resistance of about 20N/m at 120kph, while Equation (5.3) implies an increased rolling resistance of about 0.3N/kg. Increasing the rolling resistance by 50% to allow for the other effects listed in Section 5 and equating the forces gives a ‘break even’ covering mass of about 40kg/m. However, usually the wagon will be loaded; if it is unladen for 10% of the time the ‘break even’ covering mass drops to 4kg/m. This is equivalent to a steel skin that averages about 0.2mm thick, probably too thin to survive arduous service, but it could be produced from

readily available sheet; the economic viability would depend on design, manufacture, compliance, installation, and maintenance costs.

American work (e.g. [9]) has predicted large savings from optimising the aerodynamics of freight trains “fuel savings … 1 gallon per mile per train” [7]. Assuming the engine is 40% efficient and that diesel has an energy density of 44MJ/kg and a density of 832kg/m^3 one gallon per mile is equivalent to 346MJ per mile, which (at an average wind speed of about 4m/s and using measured train speed) from Fig 9 is equivalent to the optimal positioning of about 25 containers. This is a reasonable number of containers to be in poor positions and gives added confidence in the results presented here.

9 Conclusions

Equations have been developed that enable the effect on energy consumption of container position within a freight train to be estimated. The equations have been used to compare two container layouts and illustrate the benefits that could be expected under different wind conditions.

The analysis indicates that previous work on freight aerodynamics that ignored both the effect of end vehicles in a rake and the effect of crosswinds would have reached valid conclusions (at around average wind speeds the two effects cancel each other).

A comprehensive assessment of measured data on freight trains supplied by Freightliner Ltd has been carried out. This showed that the energy saved by optimal positioning of any single container is equivalent to that saved by transporting a load that is reduced by only 54kg. If future freight speeds were to increase the savings would become more significant due to the speed squared term in the air resistance calculation.

Acknowledgements

The authors would like to thank Armando Carrillo Zanuy for his help in obtaining source material and Freightliner Ltd for data on container traffic.

This work was supported by the EC Framework 7 project SustRail: “The sustainable freight railway: Designing the freight vehicle – track system for higher delivered tonnage with improved availability at reduced cost”, Grant 265740.

References

[1] Vollmer G. Luftwiderstand von Guterwagen (Air resistance of goods wagons). Darmstadt; 1989. German.

[2] ISO. Standard Atmosphere. International Standards Organisation; 1975. 2533.

[3] Wende D. Fahrdynamik des Schienenverkehrs (Dynamics of rail transport). Teubner Verlag; 2003. German.

[4] Carrillo Zanuy A, Kendra M, Camaj J, Mašek J, Stolz S, Márton P. D 2.1 Intermodal application of VEL-Wagon. Versatile, Efficient and Longer Wagon for European Transportation (VEL-Wagon); 2011.

[5] Lindgreen E, Sorenson SC. Driving Resistance from Railroad Trains. Technical University of Denmark; 2005. Workpackage 700: Emission Estimating Methodology for Rail Transport, ARTEMIS: (Assessment and reliability of transport emission models and inventory systems), Project funded by the European Commission within the 5th Framework Research Programme.

[6] Nolte R, Wurtenberger F. EVENT: Evaluation of Energy Efficiency Technologies for Rolling Stock and Train Operation of Railways. Institute for Future Studies and Technology Assessment (IZT Berlin); 2003. International Union of Railways.

[7] Engdahl RA. Full-scale rail car testing to determine the effect of position-in-train on aerodynamic resistance. [Washington, D.C.]; Chicago, Ill.: Association of American Railroads, Washington Systems Center; 1987.

[8] Watkins S, Saunders JW, Kumar H. Aerodynamic drag reduction of goods trains. Journal of Wind Engineering and Industrial Aerodynamics. 1992;40(2):147 – 178.

[9] Lai YC, Barkan CPL, Önal H. Optimizing the aerodynamic efficiency of intermodal freight trains. Transportation Research Part E: Logistics and Transportation Review. 2008;44(5):820 – 834.

[10] CEN: European Committee for Standardization. Railway applications. Aerodynamics. Requirements and test procedures for cross wind assessment. British Standards Institution; 2010. BS EN 14067-6.

[11] Golovanevskiy VA, Chmovzh VV, Girka YV. On the optimal model configuration for aerodynamic modeling of open cargo railway train. Journal of Wind Engineering and Industrial Aerodynamics. 2012 Aug;107-108(0):131–139.

[12] Jong JC. Analytical solutions for predicting train coasting dynamics. Proceedings of the Eastern Asia Society for Transportation Studies (EAST). 2003 October;4:91–103.

[13] CEN: European Committee for Standardization. Eurocode 1: Actions on structures. General actions. Wind actions. British Standards Institution; 2005. BS EN 1991-1-4:2005+A1:2010.

[14] Rail Accident Investigation Branch. Detachment of containers from freight wagons near Cheddington and Hardendale 1 March 2008. Department for Transport; 2009. 12/2009.

[15] George SE. United Kingdom Windspeed, Measurement, Climatology, Predictability and Link to Tropical Atlantic Variability. Department of Space and Climate Physics, Benfield Hazard Research Centre, University College London; 2006.

[16] SustRail. Route summary: Track characteristics, condition and economic data. ADIF; 2012. D1.4.

Appendix: Notation

Symbol	Unit	Meaning
A	m^2	Area of the front of the train
A_r	N	Parameter in equation for rolling resistance
B_r	N	Parameter in equation for rolling resistance
C	-	Aerodynamic drag coefficient
C_{Lat}	-	Lateral aerodynamic drag coefficient
C_{Long}	-	Longitudinal aerodynamic drag coefficient
C_r	Ns/m	Parameter in equation for rolling resistance
D_r	Ns/m^2	Parameter in equation for rolling resistance
F_{lat}	N	Lateral force
F_{long_lat}	N	Longitudinal force due to the lateral force
F_{roll}	N	Rolling resistance
G	m	Length of the gap between containers
k	-	Index of even Fourier coefficients
L	m	Container length
L_{tr}	m	Length of the train
n_{axle}	-	Number of wagon axles
Red_{Long}	-	End compensation factor
V_{rw}	m/s	Speed at which wind impacts train

V_{tr}	m/s	Speed of train
α	rad	Angle between wind direction and train direction
θ	rad	Relative angle between wind direction and train direction
θ_i	rad	Wind direction to impinge on group of i trailing containers
μ	-	Rail-wheel coefficient of friction
ρ	kg/m^3	Density of air